JPE 17-5-23

https://doi.org/10.6113/JPE.2017.17.5.1363
ISSN(Print): 1598-2092 / ISSN(Online): 2093-4718

Two Vector Based Direct Power Control of AC/DC Grid Connected Converters Using a Constant Switching Frequency

Adel Mehdi†, Abdellatif Reama*, and Hocine Benalla**

†,**Faculty of Technology Sciences, University Of Mentouri Brothers-Constantine, Constantine, Algeria
*Departement of System Engineering, ESIEE Paris, Marne-la-Vallée, France

Abstract

In this paper, an improved Direct Power Control (DPC) algorithm is presented for grid connected three phase PWM rectifiers. The new DPC approach is based on two main tasks. First the optimization of the look-up table, which is well-known in conventional DPC, is outlined for selecting the optimum converter output voltage vectors. Secondly a very simple and effective method is used to directly calculate their duty cycles from the power errors. Therefore, the measured active and reactive powers are made to track their references using hysteresis controllers. Then two vectors are selected and applied during one control cycle to minimize both the active and reactive power ripples. The main advantages of this method are that there is no need of linear current controllers, coordinates transformations or modulators. In addition, the control strategy is able to operate at constant switching frequencies to ease the design of the power converter and the AC harmonic filter. The control exhibits a good steady state performance and improves the dynamic response without any overshoot in the line current. Theoretical principles of the proposed method are discussed. Both simulation and experimental results are presented to verify the performance and effectiveness of this control scheme.

Key words: Direct Power Control (DPC), Grid connected converters, Hysteresis controller, Three phase AC/DC rectifiers

I. INTRODUCTION

In recent years, three phase voltage source converters (VSCs) have been widely used in various new active systems interconnected to the grid such as active power filters, utility interfaces with non-conventional energy sources (wind turbines, photo-voltaic, fuel cells, etc.) and power quality improvement units (FACTS). Consequently, VSCs have become an important part of modern power electronics. Generally, these devices must provide a target active and/or reactive power level to the line. Therefore, appropriate power control systems are required.

The conventional control method for VSCs was proposed in [1]. A frequency domain analysis is used to obtain appropriate transfer functions to control the system synthesis [2]. With the high efficiency control applied for induction motors in [3], a new control strategy of pulse-width modulation (PWM) converters [4] can be achieved by controlling the instantaneous active and reactive powers. It uses a switching table to select the optimum output vectors without line voltage sensors. Another study [5] based on virtual flux estimation is presented and investigated under an unbalanced grid. Moreover, direct power control was improved using space vector modulation (DPC-SVM) to control PWM rectifiers with a constant switching frequency [6].

Recently, predictive approaches [7], [8] have attracted more attention for the control of VSCs with minimum distortion and harmonic noise without any overshoot. In [9], [10] the well-known direct power control is combined with predictive selection of the voltage vectors sequence. A new prediction process was proposed in [11] to predict the currents for all of the possible converter vectors, when the error signals of the system are evaluated using a cost function. This method was improved in [12] to operate with a constant switching

Manuscript received Jun. 29, 2016; accepted May 23, 2017
Recommended for publication by Associate Editor Jae-Do Park.
†Corresponding Author: adel.mehdi@lec-umc.org
Tel:+213-31-90-81-13, Fax:+213-31-90-81-13, University of Constantine
* Departement of System Engineering, ESIEE Paris, France
**Faculty of Technology Sciences, University Of Mentouri Brothers-Constantine, Algeria

frequency with no power source voltage sensors. However, this predictive current controller has a poor performance under component parameter variations [13], [14]. Therefore, to overcome this task, a control method was presented in [15], where the load resistance and inductance are estimated using the least square method of an online parameter calculation. This is done based on digitally sampled instantaneous voltage and currents.

An example of a modified switching table is presented in [16], where the DC-link voltage is regulated via fuzzy logic and a PI controller. Improved dynamic response and steady state performance has been achieved in [17] by applying a fixed switching frequency. A dead-beat direct power control strategy for the grid integration of low cost three phase PWM converters was studied in [18]. In addition, the authors of [19] discussed the control of three phase voltage source rectifiers (VSRs) with an arbitrary number of voltage levels.

The Direct Power Control (DPC) strategy can also be applied for doubly fed induction generator (DFIG) based wind turbine systems [20]. A constant switching frequency can be achieved in [21] which eases the design of the power converter and the AC harmonic filter. Three vectors are selected and applied during one control period to reduce both the active and reactive power ripples using RMS ripple minimization [22] and the dead-beat approach [23]. As a result, the switching frequency can be significantly reduced. Furthermore, shunt active power filters have been implemented using direct power control in [24], [25]. They have also been developed with sliding mode control [26] and predictive approach [27]. High Selectivity Filters (HSF) are recommended in [28] to achieve a near sinusoidal source current waveform under distorted or unbalanced grids.

The contribution of this paper to the study of PWM rectifiers connected to a network involves adapting the concept of the duty cycle, well-known in the control of the electric machines in conventional DPC, to improve the quality of electric power. This new approach of DPC can guarantee a constant switching frequency without needing to know the system parameters, like other predictive technologies. This introduces bad behavior when the parameters of the systems are varied, due to temperature changes or by other phenomena such as inductance saturation.

II. Mathematical Model

Fig. 1 presents the most popular topology. This universal topology has the advantages of using a low-cost three phase module with a bidirectional energy flow capability, and providing a unity power factor (UPF).

Fig. 2 shows a basic diagram of a three-phase boost converter. The AC side converter system can be described with the following equation:

$$V_s = Ri_s + L\frac{di_s}{dt} + V_{inv} \quad (1)$$

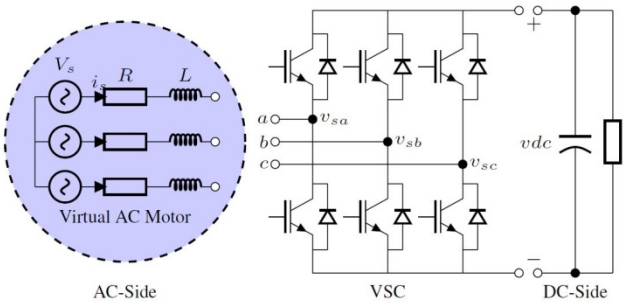

Fig. 1. Three phase PWM rectifier system.

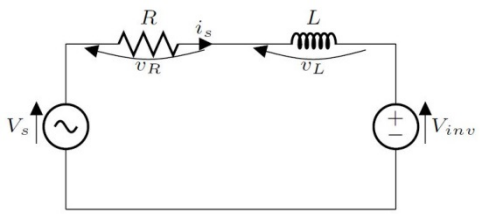

Fig. 2. Equivalent circuit of an AC/DC converter.

Where V_{inv} is the converter voltage, V_s is the AC source voltage, i_s is the line current, and R and L are the equivalent resistance and inductance between the source and the converter, respectively. The DC-link side of the PWM converter can be defined by:

$$C\frac{du_{dc}}{dt} = S_a i_a + S_b i_b + S_c i_c - i_{load} \quad (2)$$

The integration of the line voltage leads to a virtual flux vector as follows:

$$\psi_s = \int (V_s - Ri_s)dt \quad (3)$$

Then the angular position of the virtual flux can be expressed by:

$$\theta = arctan\left(\frac{\psi_\beta}{\psi_\alpha}\right) \quad (4)$$

Well-known equations of the instantaneous powers are presented in:

$$P_s = \frac{3}{2}\left(V_\alpha i_\alpha + V_\beta i_\beta\right) \quad (5)$$

$$Q_s = \frac{3}{2}\left(V_\beta i_\alpha - V_\alpha i_\beta\right) \quad (6)$$

III. Control Strategy

The DPC method is similar to Direct Torque Control (DTC) for induction motors. Instead of the torque and stator flux, the instantaneous active and reactive powers are controlled. The following figure shows a scheme of the proposed method.

The two vector based direct power control strategy presented in Fig. 3 introduces one active vector and one zero vector during one control period. This is done to minimize both the active and the reactive power ripples and to achieve a constant switching frequency. The commands of the reactive power (set to zero) and active power delivered from the outer DC voltage controller are compared with measured values, using two simple band hysteresis controllers (Fig. 6). Therefore, the

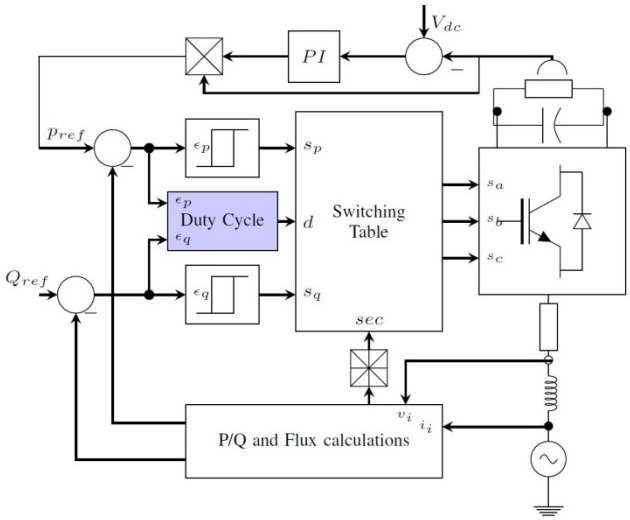

Fig. 3. Block scheme of DPC-2V.

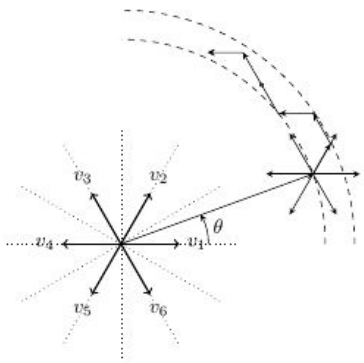

Fig. 4. Choice of the first voltage vector.

TABLE I
MODIFIED SWITCHING TABLE

s_p	s_q	θ_1	θ_2	θ_3	θ_4	θ_5	θ_6	θ_7	θ_8	θ_9	θ_{10}	θ_{11}	θ_{12}
↓	↓	6	1	1	2	2	3	3	4	4	5	5	6
↓	↑	5	6	6	1	1	2	2	3	3	4	4	5
↑	↓	1	2	2	3	3	4	4	5	5	6	6	1
↑	↑	3	4	4	5	5	6	6	1	1	2	2	3

converter switching states are appropriately selected by a switching table based on the instantaneous errors, the line voltage vector position and the duty cycle.

Applying each of the active voltage vectors (Fig. 4) to a converter causes a change in the active and reactive power values. Consequently, for each condition and each sector of the voltage plane, one of the six active voltage vectors that has the best effect is selected (Table I) the first time. Then it is combined with another zero vector taking account of the minimum variation in the switching state. For example, if the first vector is $v_1(100)$ it is combined with $v_0(000)$ and not with $v_7(111)$.

The basic idea of the proposed switching table was to choose the best rectifier voltage vector among the six possible actives vectors, as shown in Fig. 4, in order to ensure the smooth

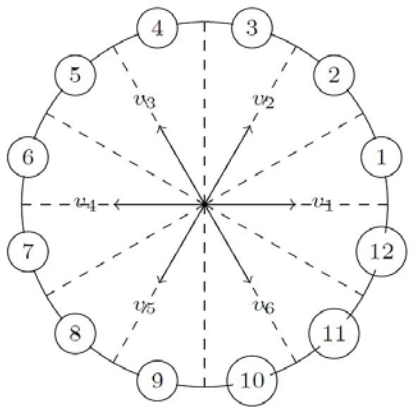

Fig. 5. Voltage vectors and sector division.

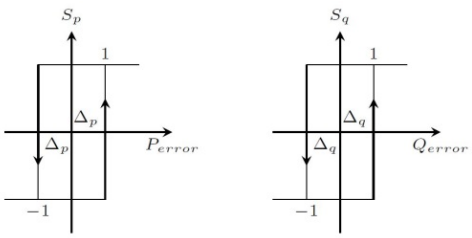

Fig. 6. Power hysteresis comparators.

control of the instantaneous active and reactive power in each sector. For this reason, the new switching table synthesis is based on the sign and magnitude of the change in the active and reactive power for each sector [29].

Assuming balanced line voltages, the rate of the active and reactive power changes in dq coordinates are presented as follows:

$$\frac{dp}{dt} = v_d \frac{di_d}{dt} \tag{7}$$

$$\frac{dq}{dt} = -v_d \frac{di_q}{dt} \tag{8}$$

The stationary coordinates are divided into 12 sectors, as shown in Fig. 5, and the sectors can be numerically expressed by:

$$(n-2)\frac{\pi}{6} \leq \theta_n < (n-1)\frac{\pi}{6}\ ; n = 1,2\ldots,12. \tag{9}$$

The output signals of the active and reactive power controllers are defined as:

$$s_p = 1 \text{ if } \varepsilon_p \geq \Delta p\ ;\quad s_p = 0 \text{ if } \varepsilon_p \leq \Delta p \tag{10}$$

$$s_q = 1 \text{ if } \varepsilon_q \geq \Delta q\ ;\quad s_q = 0 \text{ if } \varepsilon_q \leq \Delta q \tag{11}$$

Where Δp and Δq are the hysteresis bands.

Fig. 7 illustrates a steady-state waveform of the active and reactive powers during one control period for the two vector based DPC strategy.

To reduce the complexity in the duty cycle calculation of the first active vector and to improve system robustness, a simple method that does not require line parameters has been chosen. The expression of this method is given by:

$$P(k+1) = P^* \tag{12}$$

This method is based on deadbeat control. It aims to make the instantaneous active power equal to its reference value at

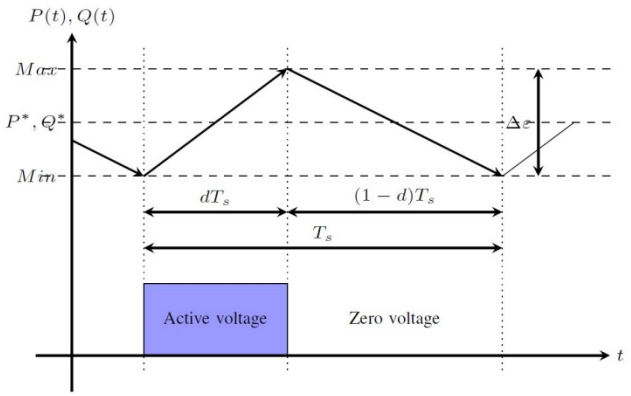

Fig. 7. Active and reactive power variation.

the end of the period cycle. Suppose that the rising slope s_1 and the falling slope s_2 of the instantaneous active power are known for the active and null vectors, as shown in Fig. 7. During a small sampling period T_s, the slopes s_1 and s_2 can be considered as constants because the dynamics of the reactive power and the DC bus voltage are not fast [30].

Under these conditions, the duration of the active vector for this method can be obtained by solving equation (12):

$$dT_s = \frac{P^* - P_0 - s_2 T_S}{s_1 - s_2} \quad (13)$$

Where P_0 indicates the initial active power value at the kth sampling instant, and d is the duty ratio of the active vector for the deadbeat control method.

A new method for obtaining the duty cycle is proposed. It eliminates the complexity and dependence of the system parameters. Before giving the expression of the new method, it is necessary to return to equation (13), which can be rewritten as follows:

$$d = \frac{P^* - P_0 - s_2 T_S}{(s_1 - s_2) T_S} = \frac{P^* - P_0}{(s_1 - s_2) T_S} + \frac{-s_2}{s_1 - s_2} \quad (14)$$

The first term in (14) is proportional to the active power error and the second term is proportional to the falling slope s_2. To eliminate the parameter dependence, it can be assumed that the denominator is constant. However, the second term related to slope s_2 is still very complex and parameter dependent. It would be natural to make the second term proportional to the error of the reactive power. Considering that the duty ratio is always positive, the final expression considered is given by the following equation:

$$d = \left|\frac{P^* - P_0}{C_P}\right| + \left|\frac{Q^* - Q_0}{C_q}\right| \quad (15)$$

Where C_p and C_q are two positive constants. Similar equation can be found in [23]. However, it was applied for DFIG control.

IV. Simulation Results

The two vector based direct power control scheme has been simulated using MATLAB/Simulink. The main electrical parameters of the power circuit and control data are given in Table II. They are the same as those for the simulations and experimental tests, except that the experimental sample time is limited by dSPACE DSP system (DS1104) at 80μs. In order to evaluate the system performance, extensive simulations have been carried out based on the proposed strategy in the steady-state and transient conditions.

TABLE II
Parameters used in the Simulation of DPC-2V

Rated power	1.0 kW
Line to line voltage (RMS)	173 V
Line frequency	50 Hz
Line resistance	2.8 Ω
Load resistance	80 Ω
DC-link capacitor	2.2 mF
Line inductance	32 mH
Constants Cp , Cq	1000
Simulation sample time	10μs
Experimental sample time	80 μs
Switching frequency	2 KHz
Dc-link voltage	270 V

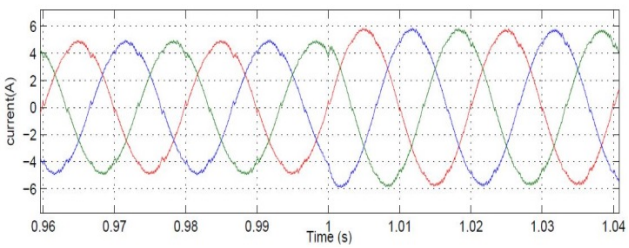

Fig. 8. Three phase line currents.

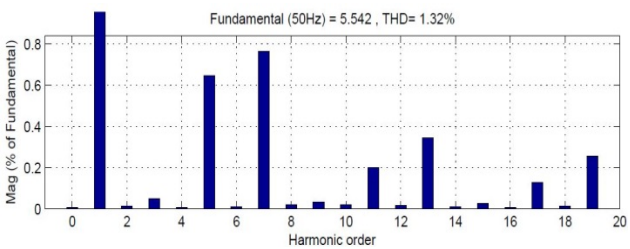

Fig. 9. Harmonic spectrum of the line current (THD = 1.32%).

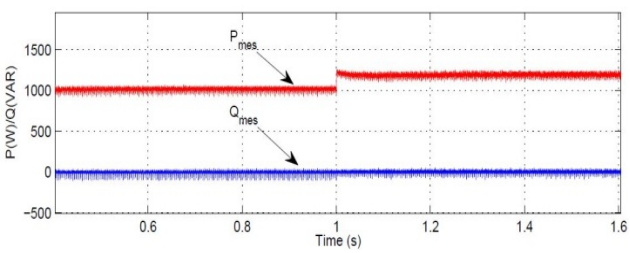

Fig. 10. Instantaneous active and reactive power.

The 2V-DPC provides a good steady-state as can be seen in the sinusoidal waveform of the line current (Figs. 8 and 9) and low total harmonic distortion ($THDi = 1.32\%$).

The simulation results confirm that algorithm meets the

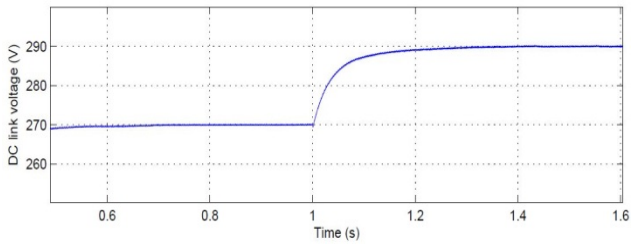

Fig. 11. Step change of the DC-link voltage.

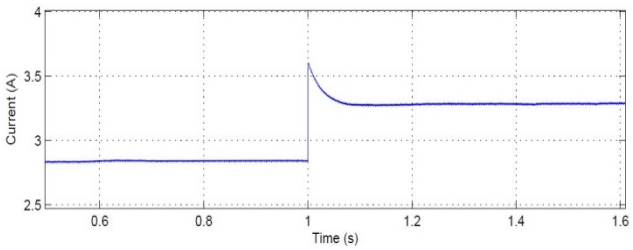

Fig. 12. Load current.

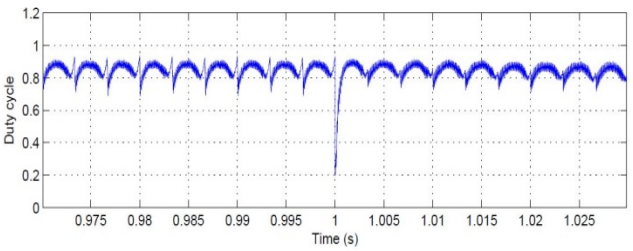

Fig. 13. Duty cycle.

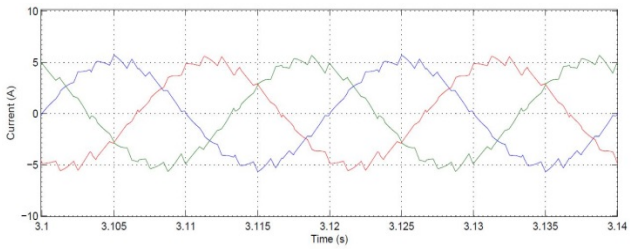

Fig. 14. Three phase line currents Fc = 800(Hz).

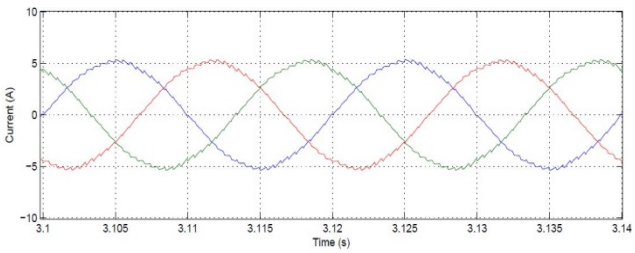

Fig. 15. Three phase line currents (L^* = 1.2L, R^* = 1.2R).

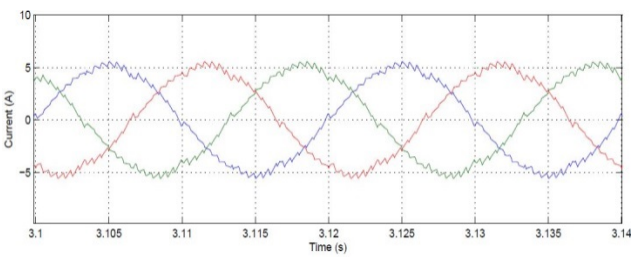

Fig. 16. Three phase line current (L^*= 0.8L, R^*= 0.8R).

IEEE standard requirements of $THDi$, which states that this value should be less than 5%.

Fig. 11 shows the transient response of the proposed 2V-DPC scheme due to a step change of the dc link voltage from 270 to $290V$ at $t = 1s$ under unity power factor operation. It can be seen that the reference value of the active power stepped up to $1200W$ (Fig. 10).

Hence, the proposed strategy also provided an excellent dynamic behavior under a step change. It can be seen that the coupling effect between the active and reactive power is practically unobservable.

This figure shows the direct current absorbed by the resistive load in the DC-link side, with an instantaneous variation at the time $t = 1s$ to react to the requested change in the voltage at the terminal of the capacitor. The rapidity of the control system is based on the Kp and Ki parameters of the PI controller dedicated to the control of the DC-link voltage.

Fig. 13 gives the duty ratio of the first active vector obtained using the dead-beat strategy, in order to reduce the instantaneous active and reactive power ripples providing a constant switching frequency.

Fig. 14 shows simulation results of the proposed DPC with a low constant switching frequency. The sampling frequency is decreased to 800 Hz and the test condition is the same as that in Fig. 8. It can be seen that the steady state performance is still acceptable considering the low switching frequency.

In this part, the robustness against line parameter variations is tested. The line resistance and inductance may differ from the values used in the control system due to the influence of temperature, magnetic saturation, etc.

The line resistance and inductance used in the control system are increased by 20% (Fig. 15) of their actual values. In the same way, the line parameters are decreased by 20% (Fig. 16).

There is no significant difference between the steady and dynamic responses when compared to the result shown in Fig. 8. This demonstrates the strong robustness to parameter variations.

The line current is stable and free of oscillations in the first case (Fig. 15). However, when a lesser inductance value is applied in the control algorithm, the system begins oscillating, as shown by Fig. 16. The change of the load current through the inductance filter must take some time if the inductance value is more important. The high stability margin is due to the independence of the duty cycle determination to parametric variations.

V. Experimental Results

An experimental laboratory setup was built in the laboratory. It consists of a commercial SEMIKRON converter controlled

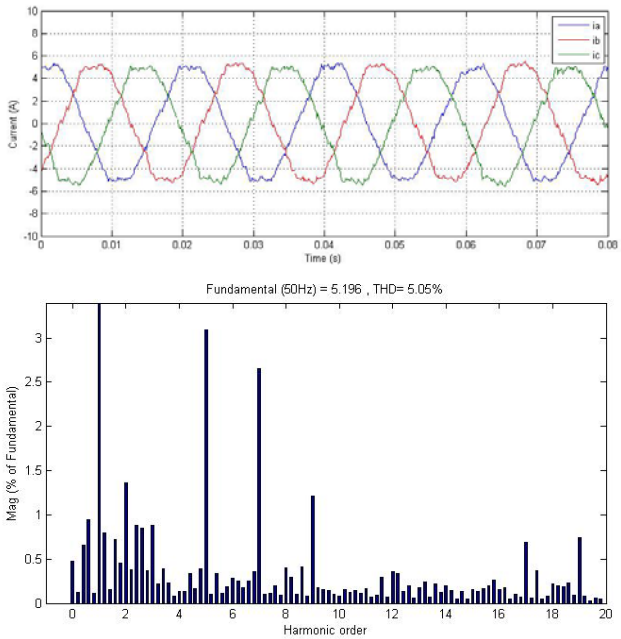

Fig. 17. Three phase line currents with specter harmonic.

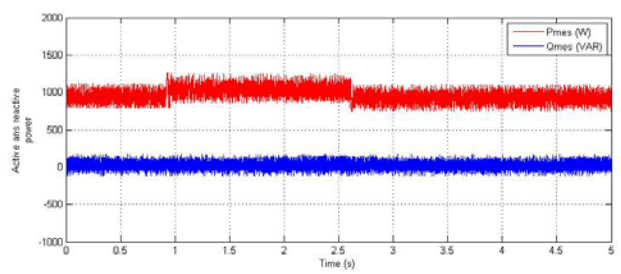

Fig. 18. Instantaneous active and reactive power.

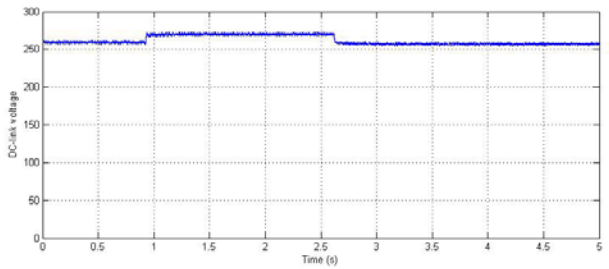

Fig. 19. Step change of the DC-link voltage.

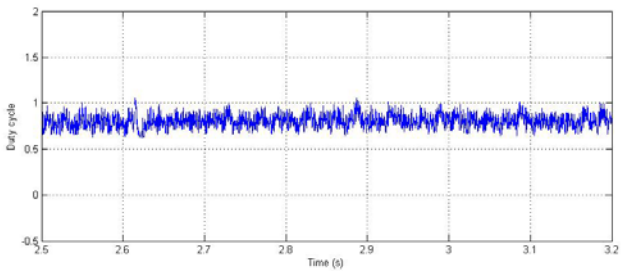

Fig. 20. Duty cycle.

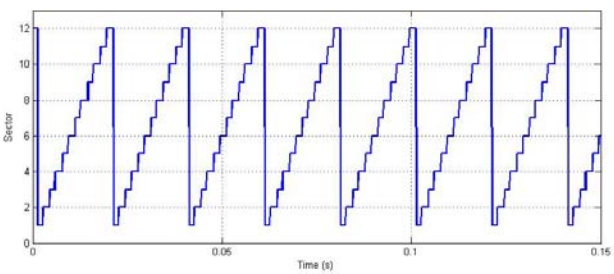

Fig. 21. Sector information.

by a dSPACE DS1104 board inserted into a PC, a variable coupling inductance in the grid side and a fixed resistor as a load. A typical lab workbench is shown in Fig. 24.

Is should be noted that the experimental results are obtained using *control desk* software incorporated with *DSpace* DS1104 package due to hardware limitations. Therefore, the data information is saved as a file in the (.mat) format. Then it is recovered and processed in Matlab to present it properly.

Fig. 17 shows experimental result of the three phase line current absorbed by the PWM voltage source converter. The 2V-DPC provides a good current waveform with a THD*i*=5.05% when using a large experimental sample time and an imperfect spectrum of the line voltage THD*v*=3.14% as shown in Fig. 23.

It can be seen from Fig. 18 that the behavior of the 2V-DPC is not very suitable due to its reduced values of the sampling frequency (80μs). The active and reactive power ripples are increased when a small sampling frequency is used in the model.

The DC link voltage increases to compensate for the real power supplied by the source. Fig. 19 shows the fast and accurate tracking of the voltage reference value.

The duty cycle calculated based on the dead-beat strategy is presented in Fig. 20. It is possible to adjust the positive constants presented in equation (12) to have more appropriate steady state and dynamic performances such those obtained with the classical PI controller.

The criteria for choosing C_p and C_q is a compromise between the dynamic response and the steady-state performance. Usually, a higher value provides less steady ripples. However, the dynamic performance is degraded. The extensive simulation results indicate that the rated power value of the system is a good starting point for C_p and C_q to achieve a good choice between the steady and dynamic performance. In other words, the duty ratio can be seen as the sum of the per unit deviations in the active and reactive power. It should be noted that the rated value of the system is just a quick starting point for C_p and C_q, and that the designer can tune them according to their specific requirements. Nevertheless, it is found that variations of C_p and C_q do not cause significant differences in the system performance [23].

Fig. 21 gives the sector information for the voltage

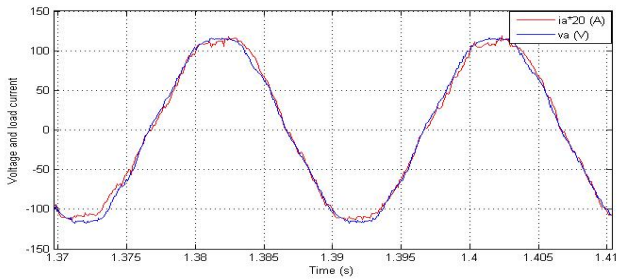

Fig. 22. Line voltage and current.

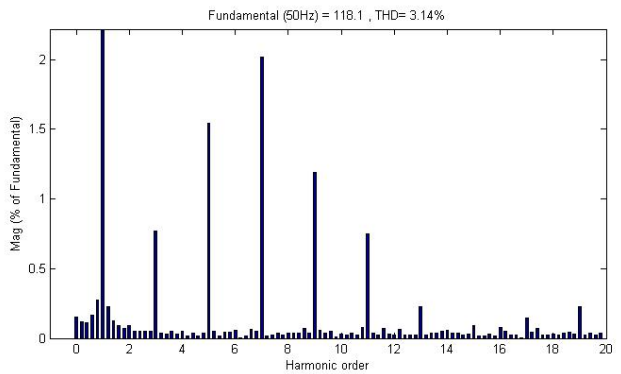

Fig. 23. Spectrum harmonic of the line voltage.

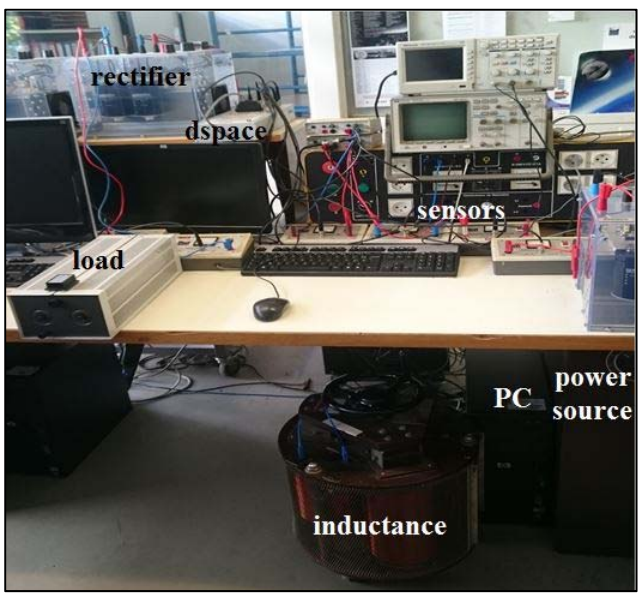

Fig. 24. Different parts of experimental test bench.

source power. The flux vectors rotate in the positive direction in the fixed reference frame. Hence, the sector number increases from 1 to 12 and resets back to 1. This is represented by the ascending staircase waveform.

Fig. 22 shows experimental waveforms of the converter output current with the grid voltage. It can be seen from this figure that the line currents are very close to a sine-wave and that they are in phase with the power source voltages.

The harmonic impedance of the electrical distribution system ensures that the harmonic currents generated by the load produce harmonic voltages (Eh =Ih x Zh). The transformers and impedance of the power supply circuits cause maximum voltage distortion for non-linear loads.

The use of non-linear loads on the utility grid and the lack of effective isolation for poor quality distribution systems may cause a non-ideal supply voltage as shown in Fig. 23. For this reason, it is preferable to use an isolation transformer to insulate the propagation of the harmonics.

VI. Conclusion

This paper has described a new direct active and reactive power control strategy for three phase PWM rectifiers, which operates at a constant switching frequency thanks to the PWM generator and to a modified look-up table applying two vectors in one control period. The duration of each vector is obtained using the power errors based the dead-beat method, which brings the benefits of simplicity and robustness against line parameter variations. The goal of this study is to alleviate the typical drawbacks of the standard DPC technique, in particular the variable switching frequency. Furthermore, steady state and dynamic tests have verified the operation and performance of the developed control process.

Finally, simulation and experimental results confirm the effectiveness of the proposed method for providing precise power control with a low total harmonic distortion (THD), and small oscillations in the active and reactive powers.

References

[1] C. Schauder and H. Mehta, "Vector analysis and control of advanced static VAR compensators," *IEE Proceedings C (Generation, Transmission and Distribution)*, Vol. 140, No. 4, pp. 299-306, Jul. 1993.

[2] M. P. Kazmierkowski and L. Malesani, "Current control techniques for three phase voltage-source PWM converters: a survey," *IEEE Trans. Ind. Electron.*, Vol. 45, No. 5, pp. 691-703, Oct. 1998.

[3] I. Takahashi and T. Noguchi, "A new quick-response and high-efficiency control strategy of an induction motor," *IEEE Trans. Ind. Appl.*, Vol. IA-22, No. 5, pp. 820-827, Sep. 1986.

[4] T. Noguchi, H. Tomiki, S. Kondo, and I. Takahashi, "Direct power control of PWM converter without power-source voltage sensors," *IEEE Trans. Ind. Appl.*, Vol. 34, No. 3, pp. 473-479, May/Jun. 1998.

[5] M. Malinowski, M. P. Kazmierkowski, S. Hansen, F. Blaabjerg, and G. D. Marques, "Virtual-flux-based direct power control of three-phase PWM rectifiers," *IEEE Trans. Ind. Appl.*, Vol. 37, No. 4, pp. 1019-1027, Jul./Aug. 2001.

[6] M. Malinowski, M. Jasinski, and M. P. Kazmierkowski, "Simple direct power control of three-phase PWM rectifier using space-vector modulation (DPC-SVM)," *IEEE Trans. Ind. Electron.*, Vol. 51, No. 2, pp. 447-454, Apr. 2004.

[7] H. M. Kojabadi, B. Yu, I. A. Gadoura, L. Chang, and M. Ghribi, "A novel DSP based current-controlled PWM strategy for single phase grid connected inverters," *IEEE Trans. Power Electron.*, Vol. 21, No. 4, pp. 985-993, Jul. 2006.

[8] S. A. Larrinaga, M. A. R. Vidal, E. Oyarbide, and J. R. T. Apraiz, "Predictive control strategy for DC/AC converters based on direct power control," *IEEE Trans. Ind. Electron.*, Vol. 54, No. 3, pp. 1261-1271, Jun. 2007.
[9] Z. Wang and L. Chang, "A DC voltage monitoring and control method for three-phase grid-connected wind turbine inverters," *IEEE Trans. Power Electron.*, Vol. 23, No. 3, pp. 1118-1125, May 2008.
[10] A. H. Bhat and P. Agarwal, "Three-phase, power quality improvement ac/dc converters," *Electric Power Systems Research*, Vol. 78, No. 2, pp. 276-289, Feb. 2008.
[11] P. Cortés, J. Rodríguez, D. E. Quevedo, and C. Silva, "Predictive current control strategy with imposed load current spectrum," *IEEE Trans. Power Electron*., Vol. 23, No. 2, pp. 612-618, Mar. 2008.
[12] P. Antoniewicz and M. P. Kazmierkowski, "Virtual-flux-based predictive direct power control of AC/DC converters with online inductance estimation," *IEEE Trans. Ind. Electron*., Vol. 55, No. 12, pp. 4381-4390, Dec. 2008.
[13] M. Monfared, H. Rastegar, and H. M. Kojabadi, "High performance direct instantaneous power control of PWM rectifiers," *Energy Conversion and Management*, Vol. 51, No. 5, pp. 947-954, May 2010.
[14] A. Bouafia, J.-P. Gaubert, and F. Krim, "Design and implementation of predictive current control of three-phase PWM rectifier using space-vector modulation (SVM)," *Energy Conversion and Management*, Vol. 51, No. 12, pp. 2473-2481, Dec. 2010.
[15] S.-J. Jeong and S.-H. Song, "Improvement of predictive current control performance using online parameter estimation in phase controlled rectifier," *IEEE Trans. Power Electron*., Vol. 22, No. 5, pp. 1820-1825, Sep. 2007.
[16] A. Bouafia, F. Krim, and J.-P. Gaubert, "Design and implementation of high performance direct power control of three-phase PWM rectifier, via fuzzy and PI controller for output voltage regulation," *Energy Conversion and Management*, Vol. 50, No. 1, pp. 6-13, Jan. 2009.
[17] D. Zhi, L. Xu, and B. W. Williams, "Improved direct power control of grid connected DC/AC converters," *IEEE Trans. Power Electron.*, Vol. 24, No. 5, pp. 1280-1292, May 2009.
[18] M. Monfared and H. Rastegar, "Design and experimental verification of a dead beat power control strategy for low cost three phase PWM converters," *International Journal of Electrical Power & Energy Systems*, Vol. 42, No. 1, pp. 418-425, Nov. 2012.
[19] G. Brando, A. Dannier, A. Del Pizzo, L. P. Di Noia, and I. Spina, "Quick and high performance direct power control for multilevel voltage source rectifiers," *Electric Power Systems Research*, Vol. 121, pp. 152-169, Apr. 2015.
[20] R. Datta and V. T. Ranganathan, "Direct power control of grid-connected wound rotor induction machine without rotor position sensors," *IEEE Trans. Power Electron*., Vol. 16, No. 3, pp. 390-399, May. 2001.
[21] D. Zhi and L. Xu, "Direct power control of DFIG with constant switching frequency and improved transient performance," *IEEE Trans. Energy Convers*., Vol. 22, No. 1, pp. 110-118, Mar. 2007.
[22] G. Abad, M. A. Rodríguez, and J. Poza, "Predictive direct power control of the doubly fed induction machine with reduced power ripple at low constant switching frequency," in *IEEE International Symposium on Industrial Electronics (ISIE)*, pp. 1119-1124, Jun. 2007.
[23] Y. Zhang, J. Hu, and J. Zhu, "Three-vectors-based predictive direct power control of the doubly fed induction generator for wind energy applications," *IEEE Trans. Power Electron.*, Vol. 29, No. 7, pp. 3485-3500, Jul. 2014.
[24] A. Chaoui, F. Krim, J.-P. Gaubert, and L. Rambault, "DPC controlled three phase active filter for power quality improvement," *International Journal of Electrical Power & Energy Systems*, Vol. 30, No. 8, pp. 476-485, Oct. 2008.
[25] A. Chaoui, J.-P. Gaubert, and F. Krim, "Power quality improvement using DPC controlled three-phase shunt active filter," *Electric Power Systems Research*, Vol. 80, No. 6, pp. 657-666, Jun. 2010.
[26] A. Djerioui, K. Aliouane, and F. Bouchafaa, "Sliding mode direct power control strategy of a power quality based on a sliding mode observer," *International Journal of Electrical Power & Energy Systems*, Vol. 56, pp. 325-331, Mar. 2014.
[27] P. Cortes, J. Rodríguez, P. Antoniewicz, and M. Kazmierkowski, "Direct power control of an AFE using predictive control," *IEEE Trans. Power Electron*., Vol. 23, No. 5, pp. 2516-2523, Sep. 2008.
[28] N. Mesbahi, A. Ouari, D. O. Abdeslam, T. Djamah, and A. Omeiri, "Direct power control of shunt active filter using high selectivity filter (HSF) under distorted or unbalanced conditions," *Electric Power Systems Research*, Vol. 108, pp. 113-123, Mar. 2014.
[29] A. Bouafia, J.-P. Gaubert, and F. Krim, "Analysis and design of new switching table for direct power control of three-phase PWM rectifier," in *13th International Conference on Power Electronics and Motion Control, (EPE-PEMC)*, pp. 703-709, Sep. 2008.
[30] Y. Zhang and J. Zhu, "Direct torque control of permanent magnet synchronous motor with reduced torque ripple and commutation frequency," *IEEE Trans. Power Electron*., Vol. 26, No. 1, pp. 235-248, Jan. 2011.

Adel Mehdi was born in Mila, Algeria, in 1988. He received his B.S. degree from the Department of Electrical Engineering and his M.S. degree in the Management and Transformation of Electrical Energy from the Faculty of Sciences and Technology, Université des Frères Mentouri Constantine 1, Constantine, Algeria, in 2009 and 2011, respectively. He is presently a Ph.D. student and a Member of the Electrical Engineering Laboratory of Constantine (LEC). In 2012, he joined the Université des Frères Mentouri Constantine 1, as an Assistant Professor in the Department of Exact Sciences. From October 2015 to March 2017, he was a Visiting Professor in the University of Paris-Est-Marne-la-Vallée (UPEM), Paris, France. His current research interests include power electronic converters, matrix converters, active and hybrid filters, the application of power electronics in renewable energy systems AC motor control, reactive power control, harmonics, and power quality compensation systems. He has been affiliated with the IEEE as a Student Member since 2012, and with the Francophone University Association (AUF) since 2011.

Abellatif Reama was born in Morocco, in 1958. He received his Ph.D. degree in Electrical Engineering from National Polytechnic Institute of Toulouse, Toulouse, France, in 1987. He is presently working as an Associate Professor in the Department of Electrical Engineering at the Université Paris-Est, ESIEE Paris, Marne-la-Vallée,

France. His current research interests include several aspects of electrical engineering with a special focus on power electronics and control design.

Hocine Benalla was born in Constantine, Algeria, in 1957. He received his B.S. degree from the University of Sciences and Technology of Oran, Oran, Algeria, in 1980; his M.S. and Ph.D. degrees in Power Electronics from the National Polytechnic Institute of Toulouse, Toulouse, France, in 1982 and 1984, respectively; and his Ph.D. degree in Electrical Engineering from the University of Jussieu, Paris, France, in 1995. Since 1996, he has been a Professor in the Department of Electrotechnics, Université des Frères Mentouri Constantine 1, Constantine, Algeria. His current research interests include active power filters, pulse width modulation (PWM) inverters, electric machines, and ac drives.